

## NON-CONTACT STRAIN AND DEFORMATION MEASUREMENT IN YARNS, ROPES AND FABRICS

J.W.S.Hearle, Tension Technology International Ltd, UK  
I. Overington, retired (Bae), UK  
M.S.Overington, Independent Consultant, UK

**ABSTRACT:** A new optical extensometer analyzer (OEA) system has been developed for non-contact strain measurement in tensile testing. Sub-pixel analysis greatly increases the resolving power over that of conventional methods. The advantages of the system are described in the first part of the paper. The second part covers application to rope and yarn testing. The third part reports exploratory studies on the application of the system to 2D and 3D effects, such as strain distribution in fabric testing and 3D buckling in fabric drape. The system is comparatively low-cost. An incidental advantage is a video-record of each test. The system has potential for monitoring fabric deformations in use.

### INTRODUCTION

For the engineering design of industrial textiles, especially if they are to be used in engineering applications, it is essential to have means of making accurate measurements of mechanical properties of fibers, yarns, cordage and fabrics. The research reported in this paper arose out of the need for Tension Technology International (TTI) to measure the load-extension properties of high-tenacity yarns with low break extensions in order to evaluate their suitability for high-performance ropes. For deepwater mooring of an oil-rig, which might use 2 km of 20 kg/m (20 Mtex) rope with a break load of 1000 tonnes, the comparatively low modulus of polyester has proved to best meet the engineering demands, but other uses require the low extension of high modulus yarns.

In tensile tests, extension is commonly recorded by the movement apart of the grips, but there is always an error due to elongation in the grip region. Major slippage, when the whole specimen in the grip moves, is usually detectable, but the inevitable localized movements merely cause the apparent strain to be greater than the true material strain. With positive adhesive bonding, there is shear in the material of the grip and the yarn; with a frictional grip, slip must occur as the friction force transfers tension to the specimen over a finite distance. The error is negligible for low-strength, high-extension specimens with a high aspect ratio (length/width), but is greater for high-modulus, high-tenacity yarns. For thick ropes, low aspect ratios increase the error in strain. Gripping is difficult because the forces are large, yarns may be difficult to bond or have low-friction finishes, and tension increases with area (radius<sup>2</sup>) but grip force increases with circumference (radius<sup>1</sup>). The use of many turns round bollards builds up a grip force, but over a long slip length.

These problems led to a need for devices to measure the elongation of part of the specimen away from the grips. Clamps linked to length measuring devices, such as LVDTs, may be used, but non-contact methods are preferable. One commercial system uses two lasers on mounts that move under servo-control to lock onto markers on the specimen. However, for the 21<sup>st</sup> century, it is better to take advantage of the advances in digital imaging. As shown by numbers given below, a simple approach based on single-pixel analysis is only of limited use. The advance described in this paper depends on the use of sub-pixel analysis, which gives a great increase in useful resolving power. The method has been successfully used on high-modulus yarns, and, subject to some development problems associated with marking the specimen, on ropes.

A later part of the paper describes exploratory studies of the use of sub-pixel analysis and special software for measurement of 2D and 3D deformations. For testing of yarns and ropes, it is straightforward to measure lateral contraction. However, fabric testing with wider specimens brings in the edge effects due to prevention of lateral contraction in the grip region. The specimen becomes waisted, and the strain varies with position. Digital imaging using the techniques described gives the potential to plot strain distributions over the specimen. Application of sub-pixel analysis to stereo-imaging, with appropriate software, provides a means of measuring three-dimensional forms, such as draped fabrics.

Some other general points should be mentioned here. For simple tensile testing, a low-cost system is available, because cheap, low-resolution video-cameras can be used. For more demanding applications, it is better to use a good digital camera. An incidental advantage in using the system in testing is that a video of the test is recorded. This can be examined at leisure to look for any anomalous effects. Finally, the potential of the system is not limited to laboratory testing; the techniques could be applied to measuring deformations of industrial fabrics in use.

## **LIMITATIONS OF CONVENTIONAL METHODS**

A critical question for optical measurement of strain and distortion is the resolution needed to give the required information. For conventional imagery, based on individual pixels, the numbers are roughly as follows. Measurement of 1% extension to an accuracy of 5%, implies a need to detect a change in length of 1 pixel in 2000 pixels. Allowing for width of the image and translation of the specimen under test, this requires analysis of at least  $2 \times 10^4$  pixels from over  $10^6$  pixels on the whole image. This is excessively large for recording, storage and analysis of time sequences. A second problem is the provision of markers on test specimens, which are suitable for routine, automated use, and not just for research studies. The ideal is clearly defined and contrasting marker edges, viewed against a constant brightness background of similar brightness to the specimen. Then automation would be relatively simple - just searching for high contrast edges orthogonal to the strain axis. In practice, it is exceedingly difficult to arrange such ideal viewing. Most situations involve spurious edges related to equipment, shadowing of the background and specular highlights on parts of the test specimen.

For most 1D studies, it is sufficient to record the absolute distance between two markers on each frame. For 3-D distortion studies, and usefully for some 2-D studies, it is necessary to compare the images in two frames. This paired frame analysis introduces the correspondence and aperture problems, studied by a research team at MIT for optical flow studies (Marr and Poggio, 1979; Hildreth, 1983; Overington, 1992). The correspondence problem results from the difficulty of unambiguously identifying locations in the images except at sharp corners. The aperture problem

states that one can only determine the motion (or displacement) of an object if the window of analysis is sufficiently large to contain the whole object.

## ADVANTAGES OF SUB-PIXEL ANALYSIS TECHNIQUES

For clean, very high contrast edges, which are aligned with an axis of an imaging system, it has been shown that the edge position can be measured to a small fraction of a pixel (e.g. MessPhysik, 1998). In an ideal situation where a pixel is crossed at right angles by a boundary between gray levels of 255 and 0 (corresponding to black and white) to give a mean gray level  $g$ , the position of the boundary would be given by  $(g/255)$ . In principle the edge location can be measured under such conditions to 0.004 pixels; in practice, there are difficulties.

- C Optical images are never razor-sharp - some finite blur results from the imaging optics.
- C Edge contrasts even approaching 255:0 are rare; the local edge gray level step is needed.
- C Straight, clean marker edges, several pixels long and aligned on vertical or horizontal axes of the imaging system are difficult to find on yarn, rope and fabric specimens.
- C Artificial edges, which are normally used, may not remain fixed on specimen locations.

However, lessons can be learnt from the highly efficient optical performance of the human eye.

- C Everyone with good eyesight (with spectacles, if worn) perceives very fine detail in images, despite the fact that the best image formed on the retina (the 'screen' at the back of the eye) has a blur circle which covers several retinal receptors (the eye's 'pixels'), Le Grand (1967), Pirenne (1967), Overington (1992).
- C For high contrast edges the ability to sense stereo disparity between image details presented to the two eyes is between 0.01 and 0.02 mrad under best viewing conditions, despite the fact that the retinal receptor matrix has at best a receptor spacing of about 0.15 mrad (i.e. a factor of the order of 10 better than the receptor spacing), Berry (1948), Overington (1992).
- C Although the sensitivity of the implied 'sub-pixel' performance is somewhat dependent on the local edge contrast in the limit, the mean positional accuracy does not seem to be impaired - i.e. the only effect of reducing contrast is an increase in the random error.

Major research some years ago into how these apparently incompatible findings could occur demonstrated conclusively that the standard human eyesight is achieved because of, rather than in spite of, the grossly blurred retinal image (Overington, 1985). This led on to the development of a computer vision system which aimed in all major respects to copy the function of the human eye and the early stages of the human visual neural system. It has been proven to yield individual pixel edge location to better than 0.1 pixels and orientation to better than 1 degree for all moderate to good contrast edges in an image and circumvents the correspondence problem (Overington, 1992). Additionally, for 3-D analysis, there is no aperture problem, provided the baseline between viewpoints is known.

The proven ability to obtain edge positional data to better than 0.1 pixels, for moderate and good contrast edges, provides a means of measuring small tensile strains and recording video clips even with simple, cheap WebCams having of the order of 150 pixels resolution. There is no great problem of high quality images. Any reasonably focused input image will do, since the first step of processing is of controlled gross blur (to simulate the gross blur occurring in the human eyeballs). With such simple recording equipment it becomes readily possible both to take, to store and to analyze

reasonably long video clips (hundreds of frames). It also becomes possible to envisage use of multiple batches of small interlinked cameras to yield stereo pairs of image streams along both horizontal and vertical stereo baselines, thus getting over the normal limitations of stereo systems for edges nearly parallel to the baseline.

## **PRACTICAL IMPLEMENTATION FOR YARN AND ROPE TESTING**

Usually elongation needs to be related to load in tests. Modern tensile testing machines are able to capture digital load readings, which can be interleaved with video-frame capture. For many older machines, load signals can be obtained through low cost analogue-to-digital (A/D) converters. Testing of high modulus yarns on old machines has demonstrated that the load readings themselves may not be absolute and may suffer from surprisingly large cyclic fluctuations arising from servo control of the crosshead. Once digitized, this kind of noise on load measurements is readily smoothed and need not interfere with determination of a clean load - elongation trace.

Implementation of the above techniques for the strain measurement in yarn testing required solution of a number of practical problems.

- C Unwanted and variable marker structure due to the method of fixing markers to the yarn.
- C Strong shadows cast on the backcloth by the clamps of the equipment holding the yarn.
- C Strong gradations of the background brightness with artificial spot lighting in some tests.
- C Bright specular highlights on some yarns.
- C Dark bands adjacent to bright yarns due to 'ringing' effects occasioned by automatic image sharpening built into the WebCam circuitry at a point prior to the first point of user access.

All the above created a need to find suitable preprocessing which compensated for the undesirable effects and/or filtered output data to reject unwanted information. We now have a sound basic sub-pixel optical extension analyzer, together with a versatile preprocessor package and a versatile output filter package which greatly increase the usefulness of the basic analyzer.

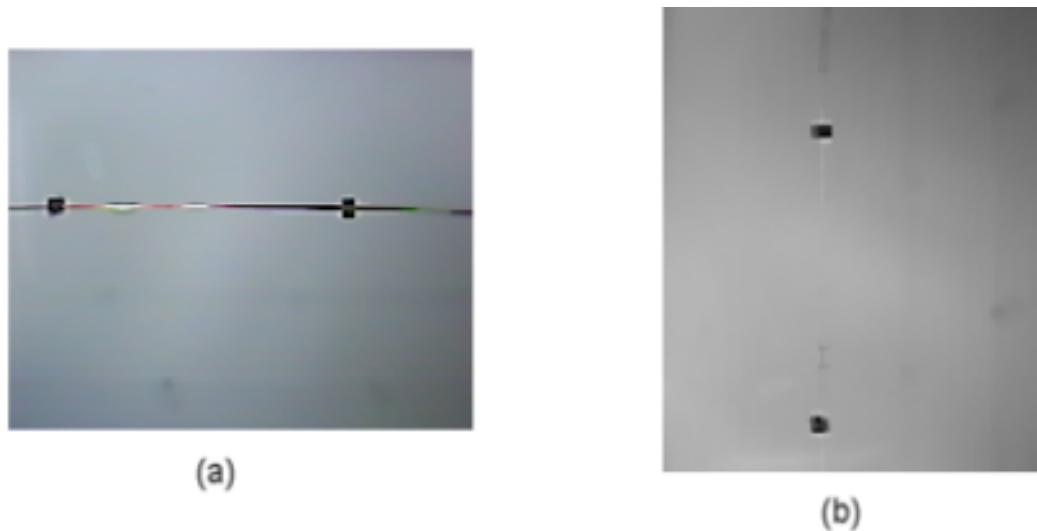


Fig. 1 : A typical frame from a yarn test video, (a) showing a number of the undesirable artifacts which frequently occur in a normal test environment, (b) the same frame after OEA preprocessing.

Our experience has shown that ideal markers for uniaxial yarn tests are short cylinders of neoprene rubber, about 6mm diameter, 5mm long and with an axial slit from the surface to the centerline. These markers work well because the material is easy to cut ‘square’, easy to peel open to attach to the yarn and virtually self-healing - so that the slit is effectively invisible during the test. Images before and after pre-processing are shown in Fig. 1. Note that the pre-processed image has been rotated. The resolution of cheap Webcams has increased since they were introduced a few years ago, but they generally exhibit a 4:3 aspect ratio. For uniaxial testing, it is beneficial to maximize the pixel information recorded for a given test, so it will often be necessary to mount the camera at 90° to the line of straining and this is readily compensated for in the subsequent analysis.

As frames are processed individually, or at most in pairs, there is no real limit to the length of video test record that can be processed, other than the storage capacity of the host PC. For polyester yarns, with break strains around 12%, a video capture rate of 15 frames per second (fps) gives around 200 frames for a break test. Fig. 2 shows an example of the sub-pixel marker edge location for a uniaxial load test on a polyester yarn. In (a) we see the full output record for all four marker edges and the entire test, the apparent resolution being limited by the recording and reproduction of the graphic; in (b) is shown the full detail of a small portion of the test for one marker edge, this being immediately available for visualization as a screen display option after any test analysis.

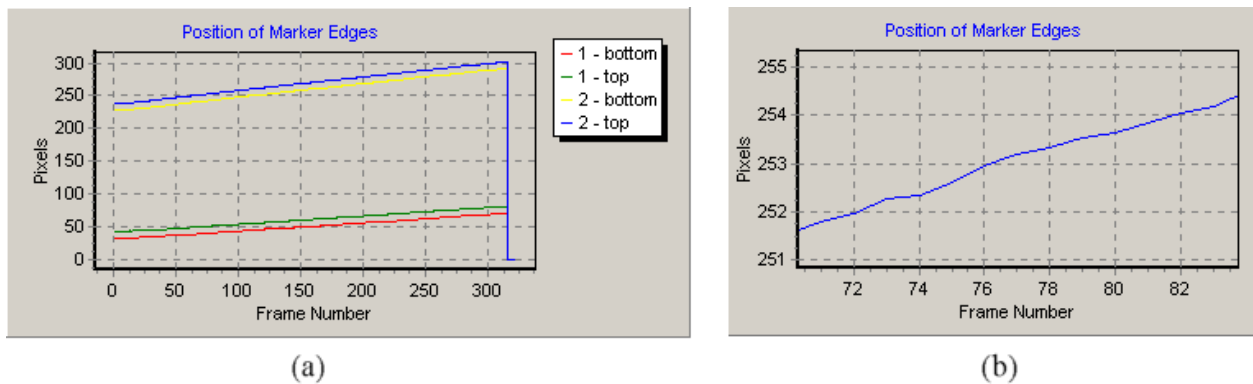


Fig. 2: Sub-pixel marker edge location for uniaxial yarn test (polyester), (a) the full test graphical output, showing positions of top & bottoms edges for the pair of markers, (b) zoomed up graphical output of a small portion of the test results, showing the sub-pixel trends for one marker edge.

Polyester has good strength and a reasonable elongation at break, it is also very easy to handle and grip, so it has become our control yarn. Fig. 3 shows the OEA load-elongation plot for the same uniaxial load test on a polyester yarn as shown in Fig. 2, where the sub-pixel marker edge locations have been utilized to give yarn strain. Note, there is no need to worry about accurately setting the marker gauge length, because this is automatically determined optically and used as the reference length for the subsequent strain determination. High-modulus yarns, such as aramids (Technora and several variants of Kevlar) and LCAP (Vectran), were easy to test reproducibly and monitor. In short break tests, it is useful to drop the WebCam resolution to 176x144 to maximize frame capture rates.

Without exception, in more than 40 separate Dyneema yarn tests, OEA plots, Fig. 4, showed a reduction in optical gauge length before the yarn started to extend. This response of Dyneema is unusual in that the strain decreases as the load increases. The only noticeable feature on the Instron trace, Fig. 5, was a curvature at the beginning of the test. It is believed that these observations, which show the advantage of detailed monitoring by OEA, are due to a combination of a real property of

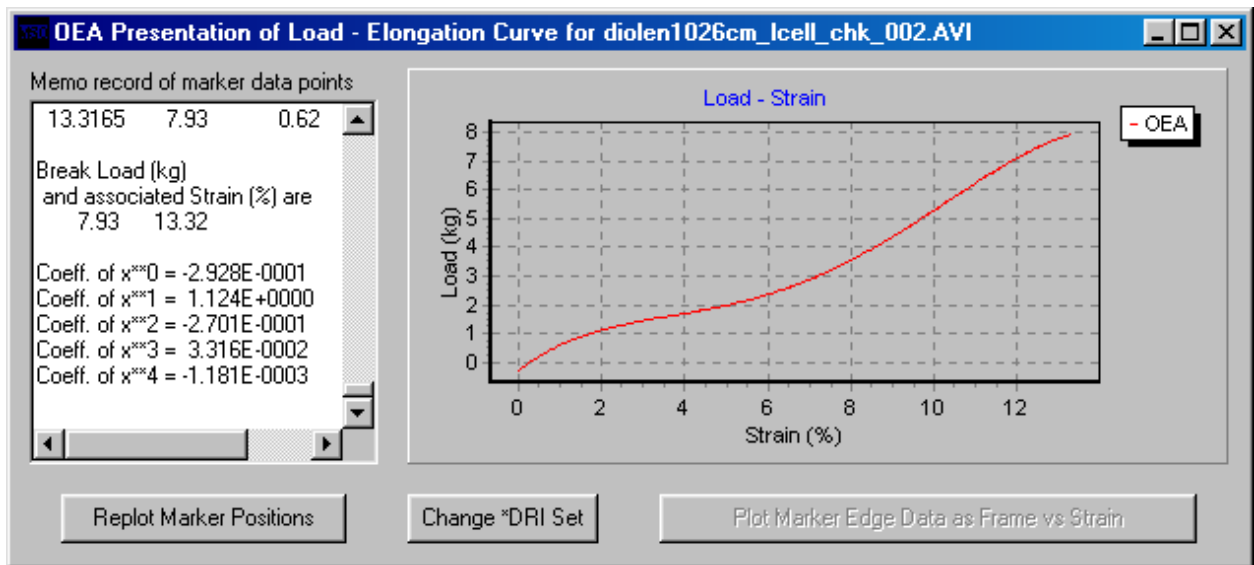


Fig. 3 : Load-elongation plot for uniaxial yarn test (polyester).

Dyneema and an artefact of testing. Retraction could occur if some molecular set in the fibers or cohesion between filaments is progressively released by the application of tension, in the same way that textured yarn from a package contracts on ‘milking’. In a true constant rate-of-loading test, this would show up as a strain reduction. In a perfect constant rate-of-extension test, there would be an increase of load as the tendency to retraction was prevented; and, once the release of set started, the consequences would be cumulative, since each increase of load would cause a further increase until the process was complete. The actual tests were nominally constant rate-of-extension, but actually constant rate-of-movement of crosshead. The tests used bollard grips. It appears that, as the crosshead begins to move, the yarn slips round the bollard, and actually realigns the grip itself. This allows the yarn between the OEA markers to contract as the load increases, thus leading to the strain reduction in the OEA trace. The increase in load would be less than in a linear trace controlled by a constant yarn modulus, which causes the curvature on the Instron trace.

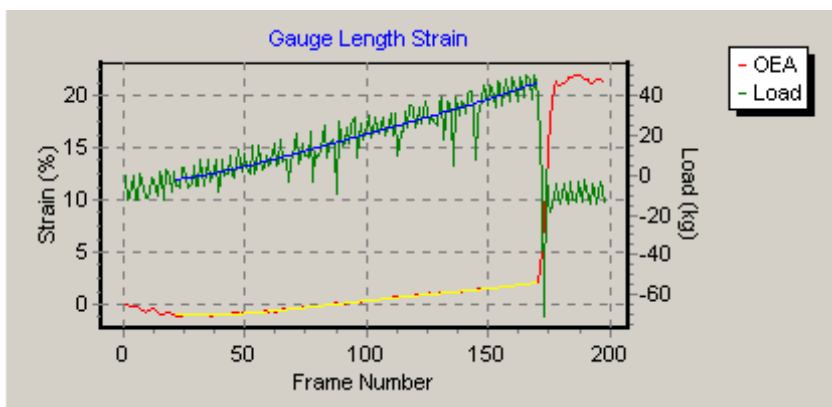


Fig. 4: OEA results for a Dyneema yarn test, with smoothing between trough strain and peak load. Upper trace shows digitized noisy analogue load signals (green) with smoothing (blue). Lower trace shows analyzed strains (red) with smoothing (yellow).

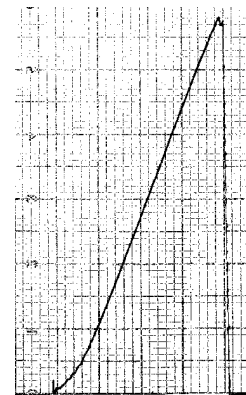


Fig. 5: Instron trace of same Dyneema yarn test.

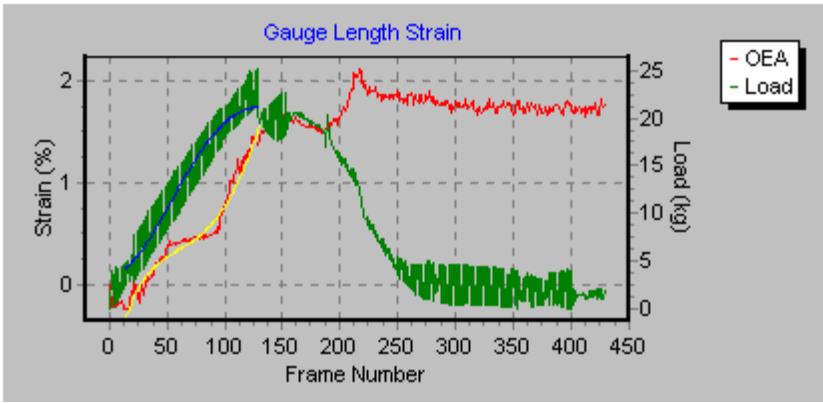


Fig. 6 : OEA trace of a resin-bonded Zylon yarn test. Load is shown in the left trace, peaking around frame 125 before falling off. The other trace shows strain, with slip between frames 50 & 100 and peaking after frame 200.

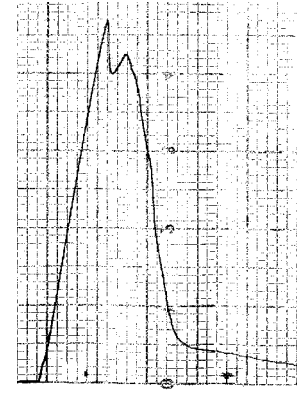


Fig. 7 : Instron trace of the same resin-bonded Zylon yarn test.

Zylon yarns were very difficult to grip. Even resin bonding failed to hold the yarn. This is shown by the slip in the OEA trace in Fig. 6. The load continued to increase as yarn slipped in the grip, and both contributions to elongation were smoothed out in the Instron trace, Fig. 7. A possible explanation of the anomalous observation that load increases despite minimal increase in gauge length strain is that one or other resin tab is slowly slipping in the jaw and releasing yarn into the test. The video record for this test does not include the jaws themselves, so this explanation cannot be verified. Peak load occurs prior to peak strain in the optical gauge length, indicating serigraphic filament breakage near the jaws.

We are just starting to collect video data for rope tests, but a first observation is that ropes are much more difficult to monitor than yarns. For testing with the commercial servo- laser system, the test laboratory had adopted the technique of fixing a pair of rigid clamps to the rope, with markers on the side faces of these clamps, as shown by the video shot in Fig. 8. In cyclic loading over a very low percentage of the rope break load, the Instron load-crosshead plots showed the expected hysteresis loops, but the servo-laser system recorded substantial sharp displacements at each reversal. OEA was used to check what was happening. The 3Com camera was set to capture video in grayscale,

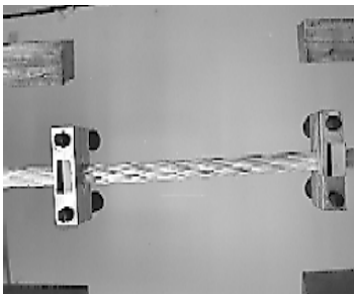


Fig. 8 : Markers on heavy duty clamps mounted on a small rope.

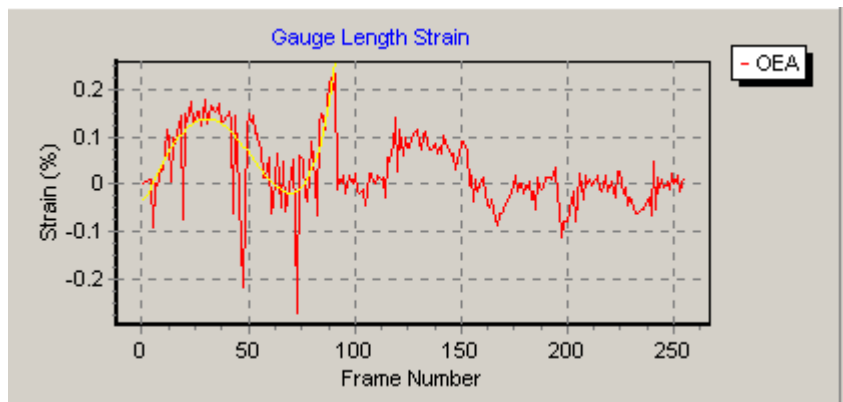


Fig. 9 : OEA trace from low strain cycling on small rope.

instead of in color, in order to maximize the capture rate on a notebook PC. Fig. 9 shows the OEA analysis of this rope test. The underlying cyclic strain can be seen at the start of the test, but there are occasional sharp spikes, considerable random fluctuation and apparent decay of the applied strain over just a few cycles. Certain errors in both recording methods are due to tipping of the clamps to give angular deflections, which appear as linear displacements of the markers, but it is obvious that the markers do not follow the applied cyclic rope strains. Work is currently in progress to find ways of marking ropes that do not lead to such errors. If clamps are used, markers need to be in the same plane perpendicular to the view direction as the rope. Alternatively, the rope may be ink marked, but ways will need to be found to overcome the disturbance of the marking by rope deformation. An advantage of OEA is that the video-record enables one to observe the movement of the clamps that leads to the false reading.

## **PAIRED FRAME ANALYSIS FOR CYCLIC AND 2-D STRAIN**

In load-elongation tests to break, strains are relatively large. The basic function of the optical image analyzer is then to measure the absolute marker position at sub-pixel level in each frame, and, from these data and the related load data, to generate stress/strain curves. In real world applications, specimens are often exposed to a large number of small strain cycles. Accurate identification of these small strains is essential for fatigue studies. It is then useful, as an alternative, to consider paired frame analysis, which computes the strain difference between two frames. A series of frames can be sequentially paired with the first frame of the cycling sequence, or any other chosen frame in the sequence, instead of relating to the zero load condition. In this way the absolute maximum sensitivity to small movements can be sensed as a time sequence over a limited deformation range, with the sampling (if necessary) chosen to suit the period of the cycles.

Thus far, although 2-D and 3-D distortions have been mentioned as theoretical concepts, the practical application of sub-pixel optical measurement techniques has been limited to our considerable experience in dealing with 1-D strain of yarns. Application to 2-D distortion of fabrics gives the potential to determine in-plane strain distributions over fabric surfaces, for example when effects such as waisting in tensile testing means that strain varies over the specimen. For 1-D strain of yarns it has proved convenient to attach markers to the yarn. Only limited information could be obtained by attaching markers to fabrics, and it is therefore preferable to monitor edges present on the fabric itself. This is where the paired-frame, optical-disparity analysis available as an optional output from within our main processor becomes a much more attractive option. Using this option, in a single analysis of a pair of frames we can obtain the component of local differential distortion orthogonal to any adequately contrasty edge in the fabric sample, subject only to two provisos.

- C Adjacent edges of similar orientation shall be at least 4 pixels apart at the image scale as offered to the main processor. For adjacent edges less than 4 pixels apart there are still recorded disparity data, but increasingly attenuated from the true value for closer edges.
- C At the scale offered to the main processor any one edge shall not have moved more than 2 pixels between the pair of frames.

Within the two above constraints, there are a wide variety of preprocessing options available in the event that one or other constraint is not met by the original pair of frames. Whilst we only guarantee accuracy to better than 0.1 pixels between frames, it should be noted that, where there are adequately extended edges, it is possible to improve on this accuracy markedly by employing conventional statistical averaging procedures on local groups of data. It should also be stressed again that the

output data are produced for every pixel containing an edge in the entire image (potentially amounting to several thousand data points at least).

The raw outputs described above are only measures of the disparity components orthogonal to the local edge orientation. This (the aperture problem referred to earlier) has to be accepted as the best one can do for these individual data points. However, we have also available some simple supplementary software which can take these output data for progressive windowed areas of the input image and from them determine automatically whether there are sufficiently varied local data in each window to circumvent the aperture problem. If so, it computes the mean differential distortion for the pair of frames (in magnitude and direction) within the said window (Overington, 1992). Given a reasonably rich and varied selection of edges in the input fabric image, this supplementary software will produce a low resolution statement of the distribution of distortion throughout the original image. This supplementary software plays off window area against effectiveness of overcoming the aperture problem so that, for any particular image pair, a best distortion map can be determined. The supplementary software can also be used to pre-process images which may not have been aligned adequately in the initial recording (Overington, 1992).

### **3-D PAIRED FRAME STEREO DEPTH DATA**

A fact apparently not widely understood, which we have found during our studies of the function of the human visual system, is that, for sub-pixel paired frame analysis of local disparities, identical processes are required, whether the paired frames are part of a time sequence, which yields optical flow maps, or a stereo pair taken at the same instant of time from two adjacent viewpoints, which yields stereo depth maps (Overington, 1992). This is important when developing a high performance image analyzer, since it means that one has available a facility not only for study of in-plane 2-D distortion, but also for study of 3-D depth distortions, such as fabric drape. The factors to be taken into account, but which there is not space to elaborate here, include the following.

- C The aperture problem can be circumvented by the extra knowledge available concerning the physical orientation of the 'binocular' baseline.
- C An alignment problem arises for local edges which are nearly parallel to the binocular baseline, because there can be no reliable disparity measurement - but this problem can be avoided by recording three images rather than two, one pair being along a horizontal binocular baseline and another being along a vertical baseline.
- C Combining the two output data sets, one arrives at a complete 3-D disparity map covering all significant local edges in the input scene.
- C Disparity itself is a rather meaningless concept in 3-D, but if a pair of images are fused on a specific distance, then the local disparities (both positive and negative) are proportional to the differences in reciprocal distances from the fusion distance.
- C Differences of reciprocal distance depend on the binocular baseline length and the field of view and resolution of the recording camera (Overington, 1992).
- C For a given camera, an appropriate set-up can cover virtually any 3-D depth simply by suitable choice of viewing distance and binocular separation.

The likely settings for study of the 3-D aspects of a fabric weave, using a typical WebCam (e.g. the 3Com Home Connect, having a field of view of around 0.76 radians and a resolution of 352 pixels) would be a binocular separation of several centimeters at a viewing distance of 10 centimeters. Study of the 3-D drape of fabric samples would probably require a binocular separation of a few

millimeters at a viewing distance of around 50 centimeters.

Although not made with OEA analysis in mind, stereo-images from a Scanning Electron Microscope (SEM) provided a way of testing 3-D edge mapping. In one example, two views of a woven fabric specimen with a small difference in tilt were digitally recorded as red and cyan components of a full color image. By separating the red and cyan images as grayscale images, scaling them down by a factor of 4 and carrying out a paired frame analysis on the reduced images, we were able to determine that there was a mismatch between the two images of approximately 2 pixels each in X and Y. A paired frame analysis was then carried out on grayscale representations of the pair of red and cyan images with appropriate repositioning. This converted the qualitatively subjective 3D view of the fabric into a quantitative listing of heights over the XY plane. The resulting disparity output was used to generate a bitmap where zero was represented as gray level 128 and the edge disparities from +2 to -2 pixels were represented as gray levels between 255 and 0. This showed clearly the grayscale representation of 3-D interlacing of the individual yarn strands in and out of the plane of the fabric. Such bitmaps provide for both subjective appraisal by viewing on a monitor and objective analysis using suitable commercial graphics programs.

A more elaborate example of 3-D edge mapping is presented as Fig. 10. Here the starting point is a stereo pair of electron micrographs of the failed region of a fiber rope, one of which is shown at (a). The general lay of the individual fibers can be inferred by visual inspection from crossovers and shading. Paired frame sub-pixel analysis with optimum fusion yields the 3-D edge map shown as (b) where the various levels of depth of the edges of the individual fibers can be seen represented as white through shades of gray to black. For Fig. 10, the depth data has been converted into gray scales. Appropriate software would allow for other forms of analysis, such as local height differences or the determination of the 3D paths of fibers or yarns. SEM views of nonwoven fabrics, which would appear similar to Fig. 10, could be analyzed to determine both in-plane and out-of-plane fiber paths.

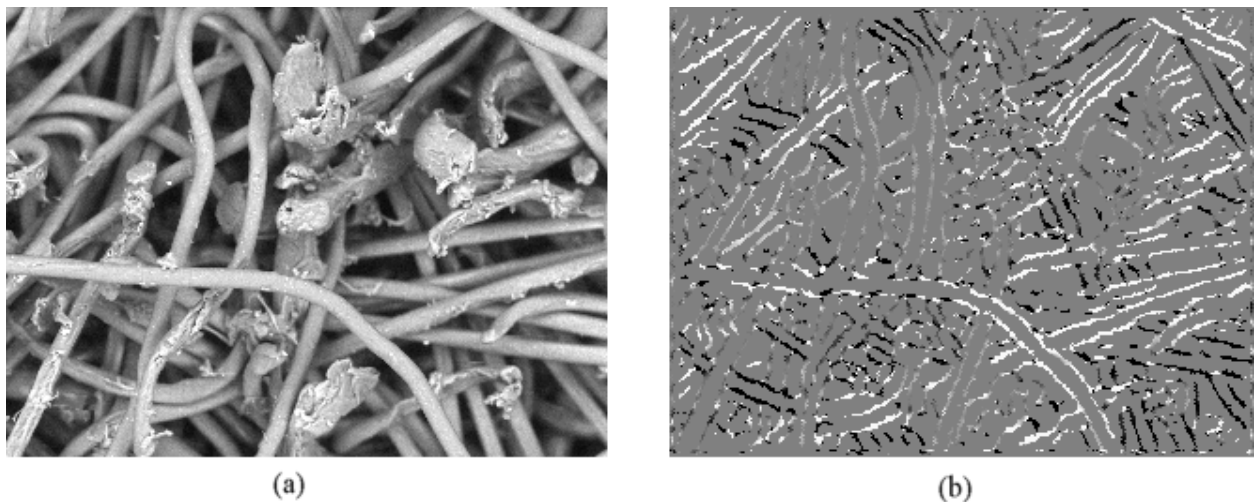


Fig. 10 : 3-D edge mapping of a failed sample from a fiber rope, (a) one of the original pair of electron micrographs, (b) the resultant 3-D edge map derived from sub-pixel, paired frame analysis.

### 3-D FABRIC FORM

The previous section is concerned with 3D structure within fabrics from high-resolution images.

Low-resolution stereo-images can be used to study the overall 3D form taken up by fabrics. Provided that the original edge distribution is adequately rich, one can generate essentially complete low resolution stereo disparity maps of entire input images. The resulting bit-map images can be visualized as gray scale pictures where zero disparity is represented as an intermediate gray level (usually 128), the positive and negative disparities being represented as progressively lighter and darker grays from 255 to 0, i.e. white to black.

In principle, one should be able to utilize discontinuities in the fabric structure to generate the information, but we have not yet evaluated this option. A simple alternative, which could be used whether the fabric is highly patterned or rather plain, is to project a high contrast, preferably diagonal bar pattern onto the test specimen. In this case the analysis processes will preferentially sense the edges of the projected bar pattern and provide a very sound set of output data for generation of the low resolution disparity map. It has been shown that use of this technique is surprisingly insensitive to existence of local and irregular patterning and structure of the underlying fabric, thereby yielding very satisfactory 3-D disparity maps for what would otherwise be difficult viewing situations.

In Fig.11(a) we see an example of a loosely draped fabric on which a diagonal bar pattern has been projected. The fabric is at an angle to the viewing station, thus giving an opportunity for measurement of progressive depth plus local fluctuations due to the folds occasioned by the drape. Fig. 11(b) is the processed gray-scale plot. Here the distributed disparities look rather like natural shading from a point source illumination. However, one must remember that the light and shade are pure depth data, with nothing at all to do with the input lighting distribution. The information could alternatively be presented as a contour map of the surface or a distribution of the local magnitudes of double curvature.

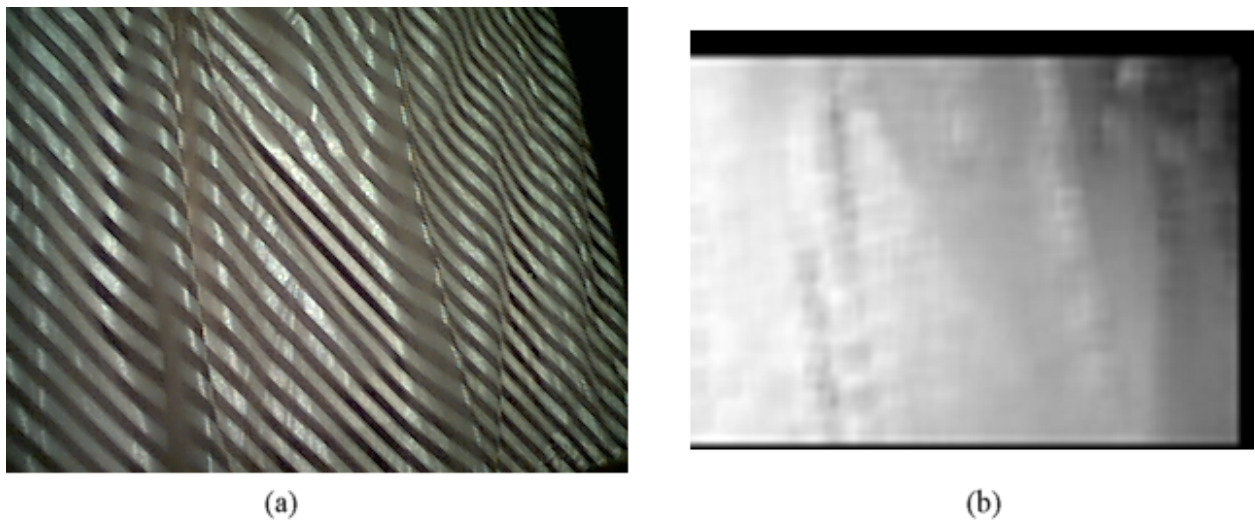


Fig. 11 : An example of generation of a 3-D surface disparity map from a relatively plain fabric by projection of a simple bar pattern onto the surface, (a) The draped material with the overlay of the projected pattern on the surface, (b) The low resolution gray coded 3-D disparity (depth) map reconstructed.

All practical experimentation on stereo to date has centered on cameras similar to the 3Com Home Connect. With maximum resolution of only around 350 pixels, the potential for wide scale analysis of either fabric structure or drape characteristics has therefore been limited by the resolution. Digital

cameras, which have now come onto the market, raise huge new possibilities for the techniques discussed. Cameras such as the Fuji 4900 Zoom, with a 6X zoom lens and resolution of 2400 x 1800 pixels, open up the possibility for either much wider scale study of fabric structure or drape characteristics from a single pair of images or for much more critical study of small fabric areas. In the limit, such new cameras have the potential to record image detail at a level equal to that achieved by the foveal (central) region of human eyes when looking through X2 binoculars! Equally, modern computers have both the speed and capacity to analyze the very large input and output files so created. High resolution images can be handled with comparative ease.

## **CONCLUSION**

Sub-pixel analysis of digital images obtained on easily available WebCams or digital cameras provides a powerful tool for measuring strains in test specimens, which avoids errors due to slip at grips. This is particularly important for high-modulus yarns with high break loads at low extensions. For ropes, where the problems of strain measurement come from the large area of cross-section and the low aspect ratio of test pieces, some further development work is needed to find good marking methods. Exploratory studies have demonstrated the potential of the technique for studying 2D and 3D deformations in testing and potentially in industrial use of fabrics. The research is a step advance in monitoring strains and overall forms of deformation, which will do much to advance an engineering approach to industrial fabric design and use.

## **ACKNOWLEDGMENTS**

The advice and assistance of Steve Banfield and Chris Towers of Tension Technology International (TTI) Ltd and financing of part of the work by TTI are gratefully acknowledged.

## **REFERENCES**

- Berry R.N. (1948), 'Quantitative relationship among vernier, real depth and stereoscopic depth acuities', *J. Exptl. Psychol.*, 38, 708.
- Hildreth E.C. (1983), 'The computation of the velocity field', MIT Artificial Intelligence Laboratory Memo. 734.
- Le Grand Y. (1967), 'Form and Space Vision', Indiana University Press, Bloomington & London.
- Marr D. and Poggio T. (1979), 'A computational theory of vision', *Proc. R. Soc. Lond. B*, 204, 301.
- MessPhysik (1998), Type ME46-250 High-resolution video extensometer with automatic target detection and operating software. Laborgeräte Ges.M.B.H., A-8280 Fürstenfeld, Austria.
- Overington I. (1985), 'A paradox - high fidelity from poor image quality', *Proceedings of Machine Intelligence '85*, IFS Publications, Bedford, U.K.
- Overington I. (1992), 'Computer Vision - A Unified, Biologically-inspired Approach', Elsevier North Holland.
- Pirenne M.H. (1967), 'Vision and the Eye', Chapman & Hall, London.